



Assessment of Pb^{2+} removal capacity of lichen (*Evernia prunastri*): application of adsorption kinetic, isotherm models, and thermodynamics

Zeynep Mine Şenol¹ · Ülküye Dudu Gül² · Selçuk Şimşek³

Received: 18 March 2019 / Accepted: 24 June 2019 / Published online: 16 July 2019
© Springer-Verlag GmbH Germany, part of Springer Nature 2019

Abstract

Biological materials play a significant role in the treatment of heavy metal-contaminated soil and wastewater. In this study, the Pb^{2+} biosorption potential of lichen *Evernia prunastri*, extensively available at a forest in Bilecik-Turkey, was investigated at batch-scale level. The optimal conditions were determined and the adsorption isotherms, kinetics, and thermodynamic calculations were also done. In order to have detailed knowledge about metal biosorption, SEM, FTIR, and BET analyses were carried out before and after the biosorption process. The optimal pH was found pH 4 and the maximum metal uptake capacity was found as $0.067 \text{ mol kg}^{-1}$. The results of this study indicate that the lichen was effectively applied to the removal of Pb^{2+} process as an inexpensive biosorbent from industrial wastewater.

Keywords Biosorption · Lichen · Pb^{2+} · Wastewater treatment

Introduction

The treatment of industrial wastewater containing a large number of heavy metals has become an important problem with the development of the industry. Particularly, the effluents of some industries such as metal plating, mining, and paper industries consist of heavy metals (Barquilha et al. 2019). These heavy metals, which are released into nature, mix with water, soil, and air, can cause serious environmental pollution problems. Also, the organisms living in polluted areas tend to accumulate these heavy metals and the accumulation of these heavy metals damage the health of the organisms. For instance, Pb^{2+} , which was a commonly used heavy

metal, can damage the central nervous system aside from the reproductive system, kidney, and liver (Salehi et al. 2014). Pb^{2+} is defined as a second class carcinogenic by WHO (WHO 2003). In contrast to organic pollutants, heavy metals are not biodegradable, so they are assumed as the environmental priority pollutants. They cause both serious environmental and health problems because of their hazardous effects. It is important to remove these toxic pollutants from industrial wastewater to protect health and the environment. Some techniques have been applied for the treatment of metal industry wastewater such as chemical precipitation, ion exchange, adsorption, membrane filtration, and electrochemical treatment technologies (Mnif et al. 2016). These methods have financial and methodological disadvantages aside from time-consuming and not environment-friendly (Mnif et al. 2015). Recently, biological treatment methods are introduced as alternatives for the removal of heavy metals from industrial wastewater due to their low-cost and eco-friendly nature (Salman et al. 2019).

In the literature, fungi and algae have been widely used in biological treatment methods and successful results have been obtained (Baysal et al. 2009; He and Chen 2014; De Rossi et al. 2018; Daneshvar et al. 2018). Lichens are the association of fungi (called as mycobiont) and green algae or cyanobacteria (called as photobiont) in a symbiotic relationship (Uluozlu et al. 2008). Photobiont produces energy with

Responsible editor: Tito Roberto Cadaval Jr

✉ Ülküye Dudu Gül
ulkuyedudugul@gmail.com; ulkuyedudu.gul@bilecik.edu.tr

- ¹ Zara Vocational School, Department of Food Technology, Cumhuriyet University, 58140 Sivas, Turkey
- ² Vocational School of Health Services, Biotechnology Application and Research Center, Bilecik Seyh Edebali University, 11230 Bilecik, Turkey
- ³ Faculty of Science, Department of Chemistry, Cumhuriyet University, 58140 Sivas, Turkey

photosynthesis for mycobiont during mycobiont supplies water and physical protection to the photobiont (Nash 2008). Lichens are showed as the indicator of heavy metal pollution of the air according to the literature due to their metal binding and accumulating capacity (Bajpai et al. 2011). However, there are a limited number of articles about the use of lichens in biological wastewater treatment, which are the example of the symbiotic lifestyle of fungi and algae. There are studies in the literature on the use of lichens as bioindicators in order to determine air pollution in environments where there is a deposition of heavy metals in the air (Beyaztaş 2008). Chettri et al. (1997) compared the ability of living and dead *Cladonia thalli* biomass to accumulate heavy metals such as Pb^{2+} , copper, and zinc from aqueous solutions. According to the results of this study (Chettri et al. 1997), the accumulation of Zinc was higher with live biomass than dead biomass. Chettri et al. (1998) showed that copper, zinc, and Pb^{2+} affected the chlorophyll structure of *Cladonia convoluta* and *Cladonia rangiformis* lichens. In recent years, Kılıç et al. (2014) studied the removal of zinc (II) ions of *Pseudevernia furfuracea* lichen by biosorption. According to the results of this study, 92% zinc (II) removal was performed by the lichen from aqueous solutions.

About 20,000 lichen species are investigated in the flora of worldwide, and 1000 of them are reported in Turkey (Aslan et al. 2006a). Since lichens have a very rich flora and are widespread in this region, most of the researchers are interested in this unique flora (Aslan et al. 2004; Aslan et al. 2006b). In the last decades, most of the studies aimed to use lichens as low-cost biomonitors to monitor the impact of toxic metals on the environment (Bajpai et al. 2011). Nevertheless, there was not any report about the utilization of lichens widespread in the Bilecik province for the removal of toxic heavy metals from aqueous solutions. For this purpose, the investigation of the biosorption capacity of lichens gains importance and also the easy availability of lichens from the region provides advantages such as reducing the cost of the process. The usage of lichens in monitoring heavy metal pollution in the air is related to the affinity of lichens to the metal-rich substrates. According to this reason, it is expected that lichens perform high metal biosorption potential from aqueous environments. Also, it is reported that lichens can tolerate high amounts of heavy metals in the air (Kılıç et al. 2014). So this metal resistance of lichens ensures high attraction on the usage of lichens to the treatment of metal-contaminated water samples. The lichen biomass is natural, easily available, and also low-cost material for biosorption of heavy metal ions. Therefore, the usage of lichen biosorbent has been shown to provide an economic solution for the removal of heavy metals from aquatic environments. This biological material was chosen as biosorbent in the study. The aim of the present study was to investigate the usage of *Evernia prunastri* biomass, which was obtained from the Bilecik province (Turkey), as a

biosorbent for the removal of Pb^{2+} from an aqueous solution. Also, it is intended to determine the optimal biosorption conditions and calculate the biosorption isotherms and kinetics models. To the best of our knowledge, this is the first report attempting to investigate the Pb^{2+} biosorption of lichen *Evernia prunastri* obtained from the Bilecik province (Turkey).

Materials and Methods

Reagents

In order to examine the biosorption of Pb^{2+} ions onto the lichen, $Pb(NO_3)_2$ and 4-(2-pyridyl azo) resorcinol (PAR as a complexing agent in spectrophotometric measurements of this ion) and other chemicals were obtained from Merck (Germany). All used chemicals were at analytical reagent grade. Double deionized water was used through the experiments and all experiments were always performed in duplicates.

Biosorbent preparation

Evernia prunastri is also defined as “oakmoss” because this lichen is located on the bark of oak trees. This lichen was reported as the most common epiphytic lichen (Yazici and Aslan 2006). In this study, *Evernia prunastri* was used for the assessment of Pb^{2+} biosorption capacity. The lichen samples were collected from the urban forest of the Bilecik province (N 40° 11.5262', E 29° 57.962') in September 2018 and were used to prepare as dried biosorbent. The lichen samples were divided from oak bark under the binocular microscope (Primo Star Zeiss) and cleaned by washing with double distilled water. In order to prepare lichen biosorbent, the biomass was dried at 70 °C over one night, then ground to make powder. To ensure that all of the powder particles were of equal size, they were passed through a 0.5-mm sieve and made ready for the experiments.

Biosorption assays

Biosorption studies were investigated in terms of pH, biosorbent amount, concentration, kinetic (time), thermodynamic (temperature), and desorption. The experiments were carried out at a shaking rate of 140 rpm in 10-mL polypropylene tubes containing 100 mg biosorbent at a constant concentration of 500 mg L⁻¹ (2.4×10^{-3} mol L⁻¹) Pb^{2+} in 10 mL solutions. The detailed explanations about experimental conditions are given in Table 1. To examine the effect pH, the variety of initial pH values (pH = 1–5) in the fixed concentration of Pb^{2+} solutions was used. In order to investigate the effect of biosorbent dosage, different amounts of lichen

Table 1 Experimental conditions for biosorption of lead (Pb²⁺) onto lichen

Experimental conditions					
Aim of experiment	Solution pH	Initial Pb ²⁺ conc. (mg L ⁻¹)	Biosorbent dosage (g L ⁻¹)	Contact time (min)	Temperature (°C)
Effect of pH	1.0–5.0	500	100	1440	25
Effect of biosorbent dosage	4.0	500	10, 50, 100, 200, 300	1440	25
Effect of concentration	4.0	25–1000	100	1440	25
Effect of time	4.0	500	300	2–1440	25
Effect of temperature	4.0	500	100	1440	5, 25, 40
Recovery	4.0	500	100	1440	25

samples as 10, 50, 100, 200, and 300 mg were tested at a constant concentration of Pb²⁺ solution. The effect of metal concentration experiments was carried out by adding 25–1000 ppm (0.12–4.8) × 10⁻³ mol L⁻¹ Pb²⁺ into the working solutions. The kinetic studies were performed in working 30 mL solutions at a constant concentration of Pb²⁺ ions containing 300 mg of lichen. The thermodynamic studies were done at 5 °C, 25 °C, and 40 °C with constant concentrations of Pb²⁺ solutions. Biosorbent-solution systems were equilibrated in a thermostatic water bath at 25 °C for 24 h and the equilibrium solutions were obtained in the aqueous phase.

Analytical methods

Pb²⁺ concentrations were determined by spectrophotometrical method (UV-VIS spectrophotometer, SHIMADZU, 160 A model, Japan) to measure the absorbance of the complex formed by PAR and Pb²⁺ ions at λ = 518.5 nm (Şimşek 2016). This spectrophotometer has a wavelength range of ± 0.2 to 2 nm within the range of 190–1100 nm. Biosorption rate (%) and biosorption amount (mol kg⁻¹) were calculated by Eqs. 1 and 2.

$$\% \text{Biosorption} = \left[\frac{C_i - C_f}{C_i} \right] \times 100 \quad (1)$$

$$Q = \left[\frac{C_i - C_f}{m} \right] \times V \quad (2)$$

In these equations (Eqs. 1 and 2), C_i is the initial concentration (mg L⁻¹), C_f is the final concentration of Pb²⁺ at equilibrium (mg L⁻¹), m is the mass of biosorbent (g), and V is the volume of working solution (L).

FTIR, SEM-EDX, and BET analysis

The functional groups on the surface of the lichen biosorbent in the absence and presence of Pb²⁺ were identified by using the FTIR technique. FTIR spectra were recorded by Perkin Elmer 400 spectrophotometer.

SEM was used to observe the 3-dimensional network structure of lichen and metal-loaded lichen samples. The surface morphology of the samples was observed with a scanning electron microscope (Leo 440 Computer Controlled Digital) equipped with an energy dispersive spectrometer (EDX) attachment.

The specific surface area and micropore volume of lichen biosorbent in the absence and presence of Pb²⁺ were measured using N₂ adsorption-desorption (AUTOSORB 1C) at -196 °C. The surface area, total pore volume, and micropore volume were determined by multipoint BET (Brunauer, Emmett, and Teller), t-plot, and DR (Dubinin-Radushkevich), respectively (El-Moselhy et al. 2017).

Results and discussion

The effect of pH on the biosorption process

The solution pH is one of the important factors affecting the adsorption process. pH is important in terms of determining the optimum conditions of adsorption as it affects the ions in the solution and also changes the load of the biosorbent surface. Most of the adsorption studies have shown that the pH of the solution affects the complex forming behavior of ions and also changes the charge of ions depending on the acidic and alkali conditions of the metal adsorption experiments (Şimşek 2016). The alkali pH values are not preferred because they cause the formation of the negatively charged metal hydroxide complexes which collapse in the adsorption working solutions. Similarly, in solutions at low pH, the cationic ions are dominant, but the positive charge of the adsorbent surface and the effect of the pushing forces between the surface and the Pb²⁺ ions cause a reduction in adsorption. For this purpose, the biosorption studies were carried out in the solutions at constant pH concentration in different pH values (1–5) and the results are given in Fig. 1.

The results show that the biosorption increased with increasing pH (Fig. 1). pH 4, which was the natural pH of the

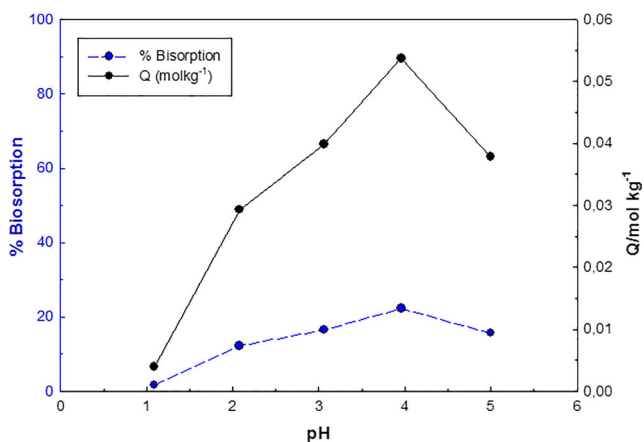
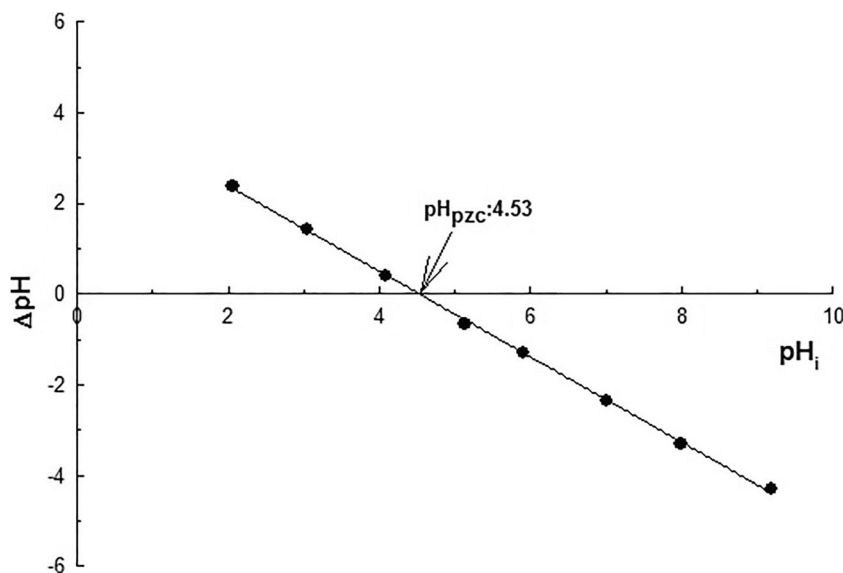


Fig. 1 The effect of pH on the biosorption ($[Pb^{2+}]_0$, 500 mg L⁻¹; biosorbent dosage, 100 mg; pH, 1.0–5.0; contact time, 24 h; temperature, 25 °C)

solution, was found as optimal pH to reach the highest adsorption rate (Fig. 1). The pH values ≥ 5 have not been studied because of the precipitation of metal ions forming hydroxides in the solutions. After the biosorption process, the final pH was measured and no significant change was observed between the initial pH and the final pH.

The solution pH is also an important parameter due to it affecting the surface charge of the adsorbent. At low and high pH values, the adsorption surface becomes positive and negative, respectively. In order to determine the surface charge and the zero charge point, the biosorbent was kept in solutions at different pH values and the equilibrium pH was measured. As seen in Fig. 2, the lichen biosorbent surface was found to be positive at pH 4.53 and became negative at further pH values. Recently, Blagojev et al. (2019) studied the effect of pH on the adsorption of Cu(II) ions by sugar beet shreds and tested only the pH values between 4.0 and 5.0; they did

Fig. 2 PZC plots of lichen



not prefer up to pH 5 due to the precipitation behavior of heavy metal ions. Blagojev et al. (2019) reported that the optimal pH for Cu(II) removal was found as 4.53 because of the functional groups on the biosorbent surface. Previously, Ekmekyapar et al. (2006) found that the lichen called *Cladonia rangiformis* Hoffm. performed maximum Cu(II) biosorption capacity at pH 5. Similarly, Baysal et al. (2009) showed that the optimal pH for Pb²⁺ biosorption on the surface of a fungus called *Candida albicans* was found at pH 5. In this study, optimal pH for Pb²⁺ biosorption on lichen *Evernia prunastri* was found as pH 4 at which the surface charge of the lichen biosorbent was positive. It was assumed that the Pb²⁺ biosorption on the lichen surface was not formed by the means of chemical interactions between heavy metal ions and the functional groups on the biosorbent surface.

The effect of biosorbent dosage on the biosorption process

Figure 3 shows the changes in biosorption rate and Q (mol kg⁻¹) values depending on the biosorbent content. As shown in Fig. 3, the increase of adsorbent dosages resulted in the augmentation of the biosorption efficiency due to the increase in the active regions. A significant increase was observed in the range of 1–25 g L⁻¹ of the biosorbent dosage. The maximum biosorption rate was found about 72% in the presence of 30 g L⁻¹ biosorbent (Fig. 3).

The effect of initial metal concentration on the biosorption process

The effect of initial metal concentration was tested with the different metal concentration varied as 25–1000 ppm. The Pb²⁺ biosorption percentage was decreased while the initial

metal concentration was increasing (Fig. 4). The metal biosorption rate was calculated as 98.87% and 55.99% at 25 and 1000 ppm, respectively. Maximum metal sorption capacity of lichen biosorbent occurred at 1000 ppm initial metal concentration as $0.075 \text{ mol kg}^{-1}$.

Biosorption isotherms

The experimental data were applied to the Langmuir, Freundlich, and Dubinin-Radushkevich isotherm models and the related parameters were derived. The Langmuir isotherm assumes that the active centers where adsorption occurs have homogeneous distribution on the adsorbent surface and the obtained experimental data are nonlinear. Langmuir equality is given in Eq. (3);

$$Q = \frac{K_L X_m C_e}{1 + K_L C_e} \quad (3)$$

In this equation (Eq. 3), Q (mol kg^{-1}) is the amount of adsorbed Pb^{2+} , C_e (mol L^{-1}) is the equilibrium concentration, X_m is the maximum adsorption capacity of the adsorbent, and K_L is the Langmuir coefficient.

The nonlinear experimental data of the Freundlich isotherm model, which provides information about the heterogeneity of the adsorbent surface, explains the hyperbolic adsorption behavior. Freundlich equality is given in Eq. (4);

$$Q = K_f C_e^\beta \quad (4)$$

In this equation (Eq. 4), K_f is a measure of adsorption capacity and β refers to the surface heterogeneity of the adsorbent.

The Dubinin-Radushkevich (D-R) model is based on the assumption that the adsorption is related to the surface

porosity and pore volume. This model is interested in energetic perspective. The D-R equality is given in Eq. (5);

$$Q = X_{DR} e^{-K_{DR} \varepsilon^2} \quad (5)$$

In this equation (Eq. 5), Q (mol kg^{-1}) is the amount of adsorbed Pb^{2+} , X_{DR} is the measure of adsorption capacity, K_{DR} ($\text{mol}^2 \text{ K J}^2$) is the activity coefficient, ε is the Polanyi potential (Polanyi potential is used as if $\varepsilon = RT \ln \left(1 + \frac{1}{C_e}\right)$), R is the ideal gas constant ($8.314 \text{ J mol}^{-1} \text{ K}^{-1}$), and E is the adsorption free energy (kJ mol^{-1}) calculated by Eq. (6)

$$E_{DR} = (2K_{DR})^{-0.5} \quad (6)$$

The E indicates the adsorption mechanism, physical or chemical. $8 < E < 16$ indicates the adsorption is chemically controlled and while $E < 8 \text{ kJ mol}^{-1}$ reveals the adsorption proceeds physically (Helfferich 1962).

Figure 5 shows the compatibility to the Langmuir, Freundlich, and D-R isotherm models, and Table 2 shows the parameters derived from these models. When the R^2 values derived from the Langmuir and Freundlich isotherm models were compared, it was found that the Pb^{2+} biosorption of lichen was better suited to the Langmuir model. This indicates that the biosorption process takes place as a monolayer of Pb^{2+} biosorption in functional groups on the surface of lichen. The maximum Pb^{2+} ion biosorption capacity for the biosorbent was $0.067 \text{ mol kg}^{-1}$ and the K_L value was 3358 L mol^{-1} . A measurement of the biosorption capacity from the Freundlich model (K_f) was calculated as 0.147 and the surface heterogeneity of β was found as 0.123. The results show that the experimental data do not fit well with the Freundlich model. The isotherm calculations of this study were supported by the previous studies. Previously,

Fig. 3 The effect of biosorbent dosage on the biosorption ($[\text{Pb}^{2+}]_0$, 500 mg L^{-1} ; biosorbent dosages, 10, 50, 100, 200, and 300 mg; pH, 4.0; contact time, 24 h; temperature, $25 \text{ }^\circ\text{C}$)

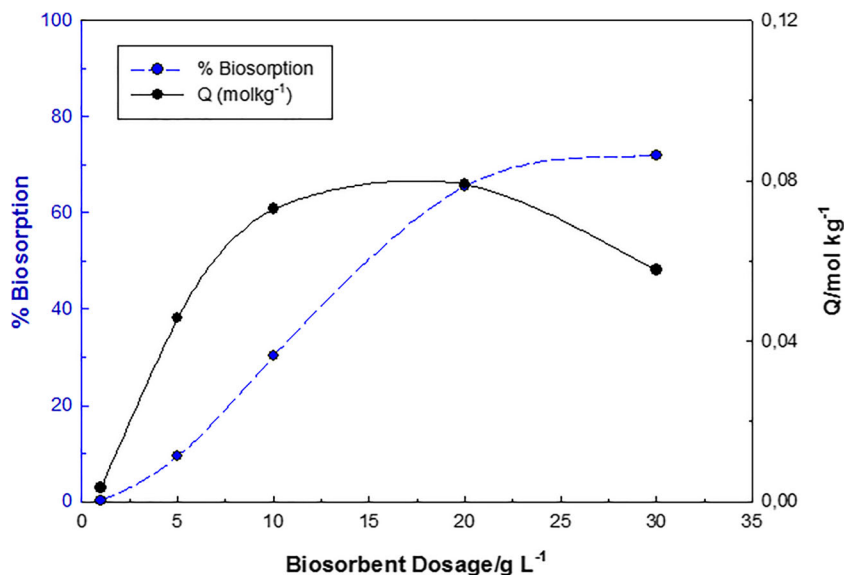
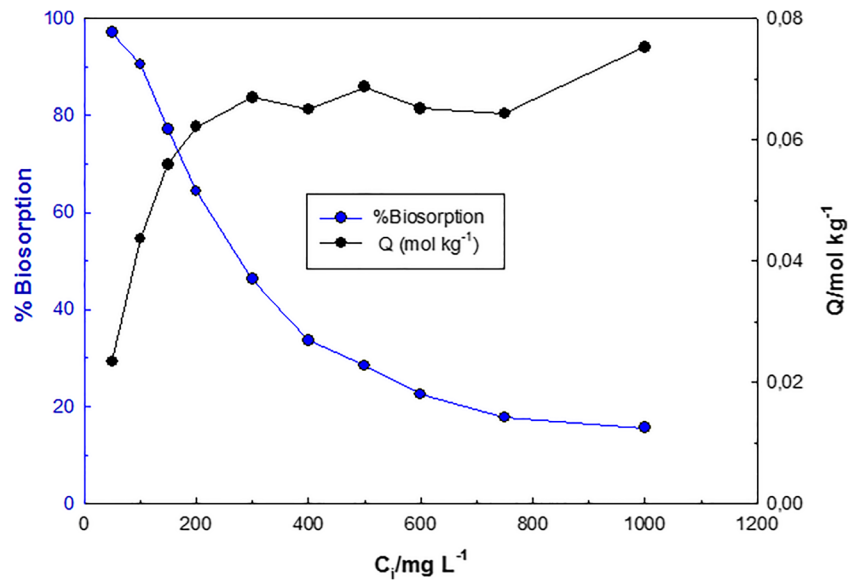


Fig. 4 The effect of initial metal concentration on the biosorption ($[Pb^{2+}]_0$, 25–1000 $mg L^{-1}$; biosorbent dosage, 100 mg; pH, 4.0; contact time, 24 h; temperature, 25 °C)



Ekmekyapar et al. (2006) showed that the Cu^{2+} biosorption on lichen *Cladonia rangiformis* was fitted with the Langmuir isotherm model. In this study, the Pb^{2+} biosorption by lichen *Evernia prunastri* was compatible with the Langmuir isotherm model. The biosorption energy from the D-R model was found to be 2.61 $kJ mol^{-1}$, which means that the biosorption process is physical.

Biosorption kinetics

Three types of kinetic models such as Lagergren pseudo-first-order, pseudo-second-order, and intra-particle diffusion

models are widely used in adsorption studies. Lagergren pseudo-first-order, pseudo-second-order, and intra-particle diffusion models were applied to the experimental data and the related parameters were derived (Fig. 6 and Table 3).

Lagergren’s pseudo-first-order equation is expressed by

$$Q_t = Q_e (1 - e^{-k_1 t}) \tag{7}$$

The pseudo-second-order equation is given as

$$Q_t = \frac{t}{\left[\frac{1}{k_2 Q_e^2} \right] + \left[\frac{1}{Q_e} \right] t} \tag{8}$$

Fig. 5 Experimentally obtained biosorption isotherms Pb^{2+} and their compatibility to Langmuir, Freundlich, and D-R models ($[Pb^{2+}]_0$, 25–1000 $mg L^{-1}$; biosorbent dosage, 100 mg; pH, 4.0; contact time, 24 h; temperature, 25 °C)

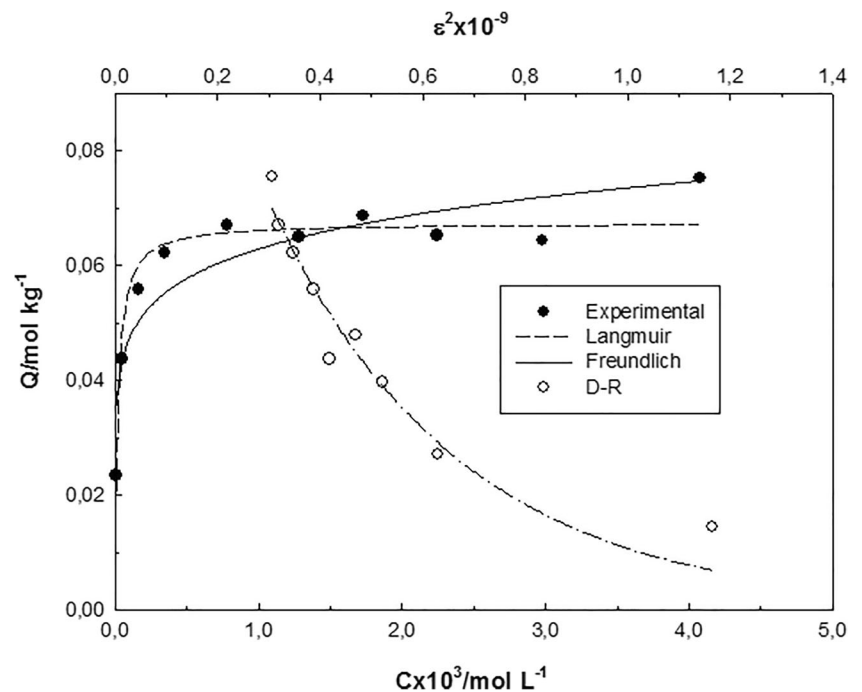


Table 2 The parameters calculated from Langmuir, Freundlich, and Dubinin-Radushkevich isotherm models

Langmuir		Freundlich		Dubinin-Radushkevich	
$X_m/\text{mol kg}^{-1}$	0.067	K_f	0.147	X_{DR}	0.066
$K_L/\text{L mol}^{-1}$	3358	β	0.123	$-K_{DR} \times 10^6$	7.11
R^2	0.928	R^2	0.848	R^2	0.648
				$E/\text{kJ mol}^{-1}$	2.6

Standard deviation $0.015 \text{ mol kg}^{-1}$, standard error $4.76 \times 10^{-3} \text{ mol kg}^{-1}$

The particle diffusion model (Weber-Morris) is given as

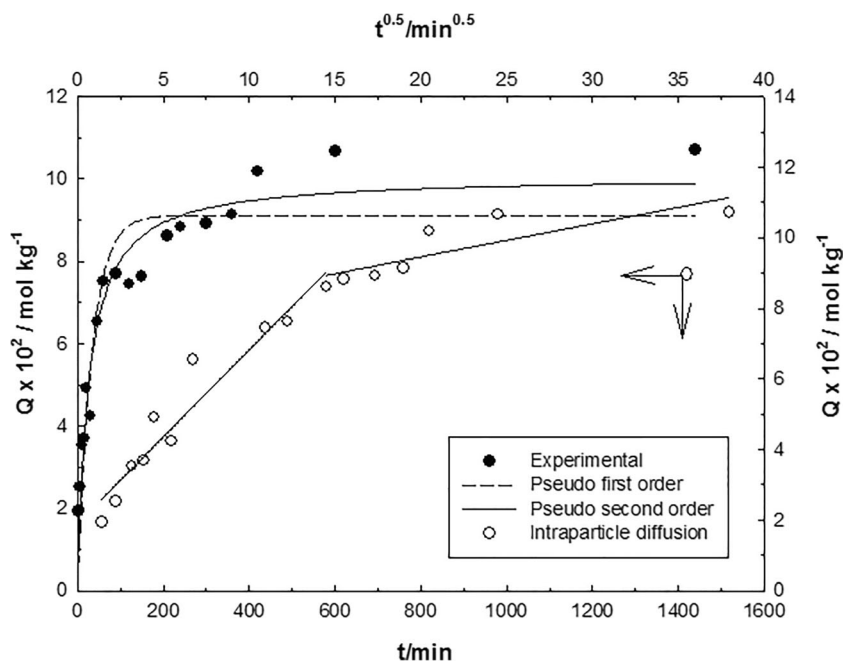
$$Q_t = k_i t^{0.5} \quad (9)$$

In these equations (Eqs. 7, 8, and 9), Q_t (mol kg^{-1}) is the amount of adsorbed ions at t time, Q_e (mol kg^{-1}) is the amount of adsorbed ions at equilibrium time, k_1 (min^{-1}) is the first-order velocity constants, k_2 (mol kg min^{-1}) is the second-order velocity constants.

The initial rate for the initial velocity was calculated using the equations of $H_1 = k_1 Q_e$ (10) and $H_2 = k_2 Q_e^2$ (11) for the pseudo-first-order adsorption and pseudo-second-order models, respectively.

Table 3 shows the values of R^2 , Q_e , and velocity constants (k_1 , k_2 , k_i). When the R^2 values were examined, it was observed that the biosorption kinetics was compatible with the pseudo-second-order model. In addition, the close approximation of the theoretically calculated Q_t and the experimental Q_e values indicates the compatibility with the pseudo-second-order model.

Fig. 6 Compatibility of Pb^{2+} biosorption kinetics to pseudo-first-order, pseudo-second-order, and intra-particle diffusion models ($[\text{Pb}^{2+}]_0$, 500 mg L^{-1} ; biosorbent dosage, 300 mg ; pH, 4.0 ; contact time, 24 h ; temperature, 25°C)



Biosorption thermodynamics

The effect of temperature on the biosorption was examined at different temperature values as 5 , 25 , and 40°C (Fig. 7). Thermodynamic parameters including enthalpy change (ΔH^0), entropy change (ΔS^0), and free energy change (ΔG^0) were calculated during biosorption. ΔG^0 free energy change was calculated with Eq. 12 (Aravindhnan et al. 2007; Slobodan 2007; Saleh and Danmaliki 2016; Rodrigues et al. 2018).

$$\Delta G = -RT \ln K_D \quad (12)$$

In this equation, R is the ideal gas constant ($8.314 \text{ J mol}^{-1} \text{ K}^{-1}$), T (K) is the temperature, and $K_D = \frac{Q}{C_e}$ is the dispersion coefficient. In this equation, the value 55.51 was used for dimensionless of K_D (Lima Eder et al. 2019).

Enthalpy and entropy parameters are calculated by using Eq. 13.

$$\ln K_D = \frac{\Delta S^0}{R} - \frac{\Delta H^0}{RT} \quad (13)$$

ΔH^0 and ΔS^0 were calculated by using the slope and cut values of the graph given in Fig. 7. ΔH^0 was found as 19.9 kJ mol^{-1} which indicates biosorption is endothermic. ΔS^0 was found as $137 \text{ J mol}^{-1} \text{ K}^{-1}$ which indicates an increase in the randomness of the biosorbent/solution interface in the biosorption process. Gibbs free energy change was calculated using Eq. 14.

$$\Delta G^0 = \Delta H^0 - T \Delta S^0 \quad (14)$$

Table 3 The calculated parameters of Lagergren pseudo-first-order, pseudo-second-order, and intra-particle diffusion models

Pb ²⁺	(k ₁ , k ₂ , k _i)×10 ³	R ²	Q _d /mol kg ⁻¹	Q _e /mol kg ⁻¹	H×10 ³
Pseudo-first order	2.73	0.864	0.091	0.102	0.28
Pseudo-second order	387	0.934	0.101	0.102	3.95
Intra-particle diffusion	4.92	0.927	–	–	–

Standard deviation 0.023 mol kg⁻¹, standard error 7.31 × 10⁻³ mol kg⁻¹

Gibbs free energy change was calculated as - 18.2, - 20.9, and - 23.0 kJ mol⁻¹ at 5, 25, and 40 °C, respectively. Negative ΔG⁰ indicates that the biosorption is spontaneous and the tendency to spontaneously increase at higher temperatures.

Recovery

Recovery/desorption of biosorbed metal is one of the most important stages of the biosorption process. A number of experiments were performed to evaluate the recovery conditions of the biosorbed Pb²⁺ ions and the results are shown in Fig. 8. As seen from Fig. 8, the maximum recovery percentage was obtained with HCl (46.2%). The lowest recovery was found in ethyl alcohol (1.4%).

FTIR, SEM-EDX, and BET analyses

Possible physicochemical interactions between Pb²⁺ ions and major functional groups of lichen in aqueous solution were characterized using FTIR analysis. As shown in Fig. 9, lichen

has some typical peaks before Pb²⁺ biosorption. The broad and strong bands at 3326 cm⁻¹ were due to a bounded hydroxyl group (-OH). The peaks observed at 2900–2960 cm⁻¹ can be assigned to the C-H group. The peaks at 1610 cm⁻¹ were attributed to the stretching vibration of a carboxyl group (-C=O). The bands observed at 1062 cm⁻¹ were assigned to CO stretching vibration of alcohols and carboxylic acids on the lichen. The peaks observed at 2921 cm⁻¹ can be assigned to the C-H group (Ekmekyapar et al. 2006; Uluozlu et al. 2008). The small variations in wave numbers were observed comparing the spectra of lichen before and after metal biosorption. This situation indicated the formation of electrostatic interactions and surface complexation between the functional groups on the surface of the lichen with Pb²⁺ ions. The FTIR analysis results proved the Pb²⁺ adsorption on the functional groups of the lichen surface.

SEM analysis is a commonly used technique to determine the differences in surface morphology of a given analyst. Figures 10 a and b show the SEM views before and after the Pb²⁺ biosorption by the lichen. As seen in Fig. 10 a and b, the lichen surface was rough prior to biosorption and was

Fig. 7 The effect of temperature on the biosorption ([Pb²⁺]₀, 500 mg L⁻¹; biosorbent dosage, 100 mg; pH, 4.0; contact time, 24 h; temperatures, 5 °C, 25 °C, and 40 °C)

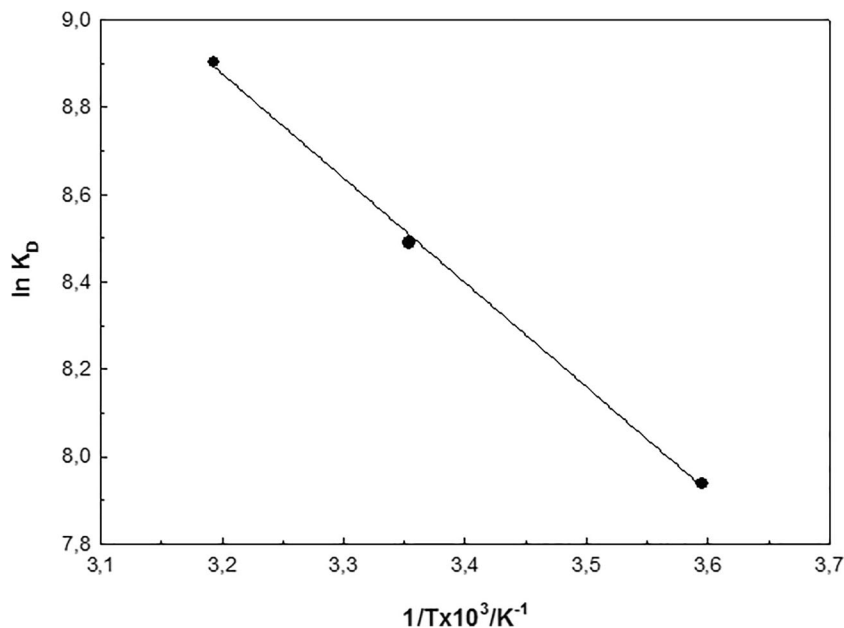
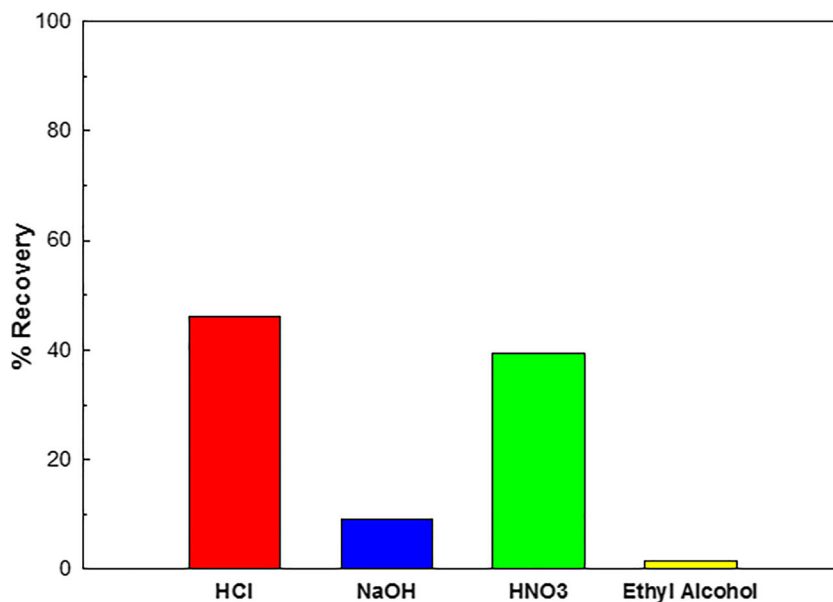


Fig. 8 Recovery percent of various solvent for desorption of Pb^{2+} ions ($[Pb^{2+}]_0$, 500 mg L⁻¹; biosorbent dosage, 100 mg; pH, 4.0; contact time, 24 h; temperature, 25 °C)

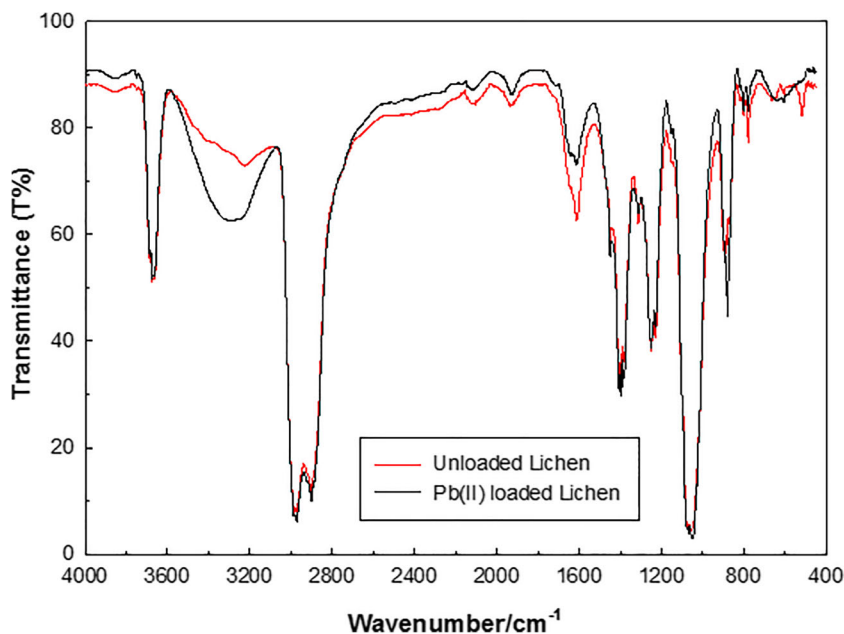


smoothed after Pb^{2+} biosorption. This may be due to the metal surface complex formation between Pb^{2+} ions and the functional groups on the surface of the lichen. Figures 10 c and d show the EDX results before and after Pb^{2+} biosorption on the lichen surface. According to the results of Fig. 10 c, lichen consists of Ca, Si, Al, and K elements as well as substantially C and O. On the other hand, the Pb^{2+} content of the lichen in Fig. 10 d was indicated the Pb^{2+} biosorption by the lichen.

Nitrogen adsorption-desorption isotherms of lichen before and after Pb^{2+} biosorption and the results of BET analysis were given in Fig. 11 and Table 4, respectively. According to IUPAC, if the pore diameter of the materials is in the range of 2–50 nm to > 50 nm, the mesopore and

macropore are defined, respectively. On the other hand, if the pore diameter is < 2 nm, the structure is defined as microporous (Kumari et al. 2006). When Table 3 was examined, it is seen that the porous diameter of lichen was < 2 nm, which indicates that lichen has a microporous structure. As seen in Fig. 11, the difference between the adsorption-desorption isotherms of lichen was small, and this indicated that the lichen had micropore structure. While the isotherms after Pb^{2+} biosorption were examined, the differences between the adsorption-desorption isotherms were gradually approaching, and this situation indicated the mesoporosity structure. Mesoporosity increased after biosorption. The increase in mesoporosity

Fig. 9 FTIR spectrum of lichen before and after biosorption of Pb^{2+} ($[Pb^{2+}]_0$, 500 mg L⁻¹; biosorbent dosage, 100 mg; pH, 4.0; contact time, 24 h; temperature, 25 °C)



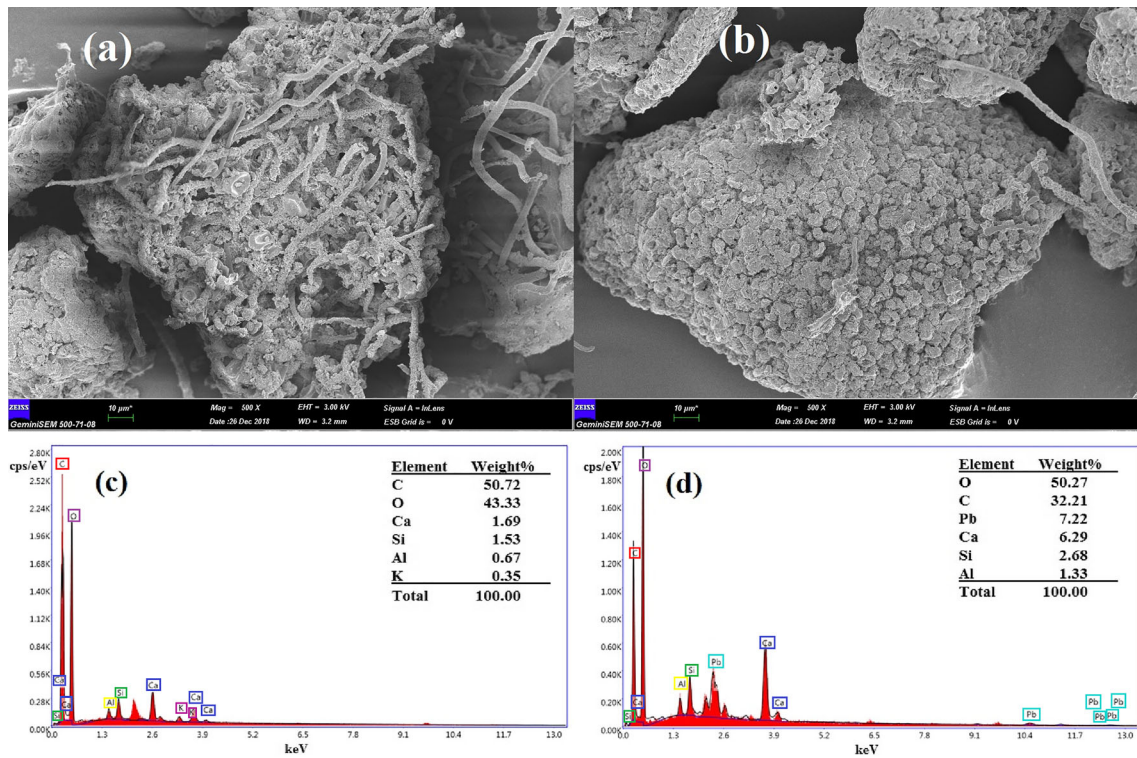


Fig. 10 SEM photographs of lichen before (a) and after (b) biosorption of Pb^{2+} and EDX results of lichen before (c) and after (d) biosorption of Pb^{2+} ($[Pb^{2+}]_0$, 500 mg L^{-1} ; biosorbent dosage, 100 mg; pH, 4.0; contact time, 24 h; temperature, 25 °C)

after biosorption was caused by the dissolved compounds such as polysaccharide, and the biosorption of Pb^{2+} resulted in narrowing the pores. Also, the SEM results were supported by the increasing porosity (Fig. 10). As given in Table 4, after the Pb^{2+} biosorption, it was observed that the BET surface area, the pore volume, and the pore diameter were increased.

According to the results of the pH experiments, the optimum pH was found to be 4 and it was found that the biosorbent surface was positively charged at the pH values lower than 4.53 with PZC experiments. These results assumed that there were no chemical interactions between positively charged metal ions and positively charged biosorbent surface at pH 4. This situation supported that the adsorption process

Fig. 11 Nitrogen adsorption-desorption isotherms of lichen before and after biosorption of Pb^{2+} ($[Pb^{2+}]_0$, 500 mg L^{-1} ; biosorbent dosage, 100 mg; pH, 4.0; contact time, 24 h; temperature, 25 °C)

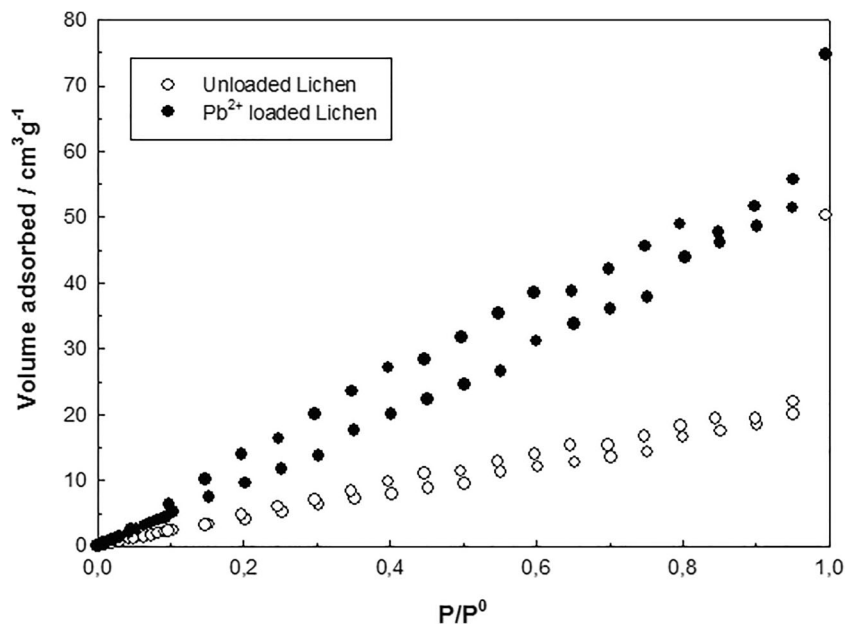


Table 4 Changes in specific surface area and pore characteristics of lichen biosorbent before and after biosorption of Pb²⁺

Sample	$S_{\text{BET}}^{\text{a}}$ (m ² g ⁻¹)	$V_{\text{Total}}^{\text{b}}$ (cm ³ g ⁻¹)	$V_{\text{micro}}^{\text{c}}$ (cm ³ g ⁻¹)	Dp (Å)
Lichen	42.6	0.0883	0.00681	7.25
Lichen-Pb ²⁺	105.4	0.1426	0.01817	7.78

^a Multipoint BET method

^b Volume adsorbed at $p/p_0 = 0.99$

^c Micropore volume calculated by DR method

was not related to chemical interactions. Similarly, the D-R isotherm calculations also indicated that the Pb²⁺ biosorption on the lichen biosorbent was physical. The results of SEM indicated that the change in the lichen surface after biosorption was caused by the binding of Pb²⁺ ions. EDX results showed that the presence of Pb²⁺ ions in the lichen structure after biosorption showed that the adsorption of the metal to the biosorbent surface was formed. Also, according to the results of BET analysis, the expansion of the pores in the lichen surface after the biosorption was considered that some polysaccharides on the lichen surface were dissolved and Pb²⁺ ions were placed in the small pores. On the other hand, FTIR results showed that there were some changes on the lichen surface after biosorption. Recently, Gurbanov and Unal (2019) reported that polysaccharides found in the cell wall of lichen (*Cladonia convoluta*) structure undergo oxidative stress when exposed to lead and the adsorption of Pb²⁺ played an important role in the band shifts to lower values according to FTIR analysis. This situation has led to significant changes in the structure of polysaccharides (Gurbanov and Unal 2019). According to the results of this study, some polysaccharide groups were found to dissolve on the surface of *E. prunastri* related to Pb²⁺ exposure. All results obtained from this study support the fact that lead adsorption on the surface of *E. prunastri* is a physical event.

Conclusion

The purpose of this study was to investigate the Pb²⁺ biosorption properties of *Evernia prunastri* and to determine the optimal conditions for the treatment of Pb²⁺-contaminated water samples by using this lichen biosorbent. Optimal operating parameters for maximum biosorption rate were determined, and the pH of the solution, the amount of adsorbent, contact time, and temperature were selected as pH 4.0, 100 g, 24 h, and 25 °C, respectively. The obtained experimental data were applied to various isotherm models and related parameters were derived. Pb²⁺ biosorption of lichen was better matched to the Langmuir model and the maximum biosorption capacity was 0.067 mol kg⁻¹. The biosorption energy from the D-R model was found as 2.61 kJ mol⁻¹, which indicated that the biosorption process was physical.

Adsorption kinetics calculations showed that the biosorption process was compatible with the pseudo-second-order model. Thermodynamic parameters ΔH^0 , ΔS^0 , and ΔG^0 showed that biosorption was endothermic, convenient, and spontaneous, respectively.

Based on all results of this study, it can be also concluded that the lichen biomass can be evaluated as an alternative biosorbent for the treatment of wastewater containing Pb²⁺ ions. The lichen biosorbent is a low-cost biomass and also performs a considerable high sorption capacity. In addition, lichen material is chosen as a novel biosorbent in this study because of it being naturally abundant, renewable, and thus a cost-effective biomass.

Acknowledgments The present study was partly supported by the Cumhuriyet University Scientific Research Projects Commission.

Compliance with ethical standards

Conflict of interest The authors declare that they have no conflict of interest.

References

- Aravindhan R, Rao JR, Nair BU (2007) Removal of basic algae *Caulerpa scalpelliformis*. *J Hazard Mater* 142:68–76
- Aslan A, Budak G, Karabulut A (2004) The amounts Fe, Ba, Sr, K, Ca and Ti in some lichens growing in Erzurum province (Turkey). *J Quant Spectrosc Radiat Transf* 88(4):423–431
- Aslan A, Güllüce M, Sökmen M, Adtgüzel A, Sahin F, Özkan H (2006a) Antioxidant and antimicrobial properties of the lichens *Cladonia foliacea*, *Dermatocarpon miniatum*, *Evernia divaricata*, *Evernia prunastri*, and *Neofuscella pulla*. *Pharm Biol* 44(4):247–252
- Aslan A, Budak G, Tıraşoğlu E, Karabulut A (2006b) Determination of elements in some lichens growing in Giresun and Ordu province (Turkey) using energy dispersive X-ray fluorescence spectrometry. *J Quant Spectrosc Radiat Transf* 97(1):10–19
- Bajpai R, Mishra GK, Mohabe S, Upreti DK, Nayaka S (2011) Determination of atmospheric heavy metals using two lichen species in Katni and Rewa cities. *Indian J Environ Biol* 32(2):195–199
- Barquilha CER, Cossich ES, Tavares CRG, da Silva EA (2019) Biosorption of nickel(II) and copper(II) ions from synthetic and real effluents by alginate-based biosorbent produced from seaweed *Sargassum* sp. *Environ Sci Pollut Res* 26:11100–11112
- Baysal Z, Çinar E, Bulut Y, Alkan H, Dogru M (2009) Equilibrium and thermodynamic studies on biosorption of Pb²⁺ onto *Candida albicans* biomass. *J Hazard Mater* 161(1):62–67

- Beyaztaş T (2008) Investigation of heavy metal pollution in lichen species *Pseudevernia furfuracea* (L.) Zopf. var. *furfuracea* from Karabük province by atomic absorption spectroscopy and rapid analysis, MSc Thesis, Ankara University, Ankara, Turkey
- Blagojev N, Kukic D, Vasic V, Sciban M, Prodanovic J, Bera O (2019) A new approach for modeling and optimization of Cu(II) biosorption from aqueous solutions using sugar beet shreds in a fixed-bed column. *J Hazard Mater* 363:366–375
- Chettri MK, Sawidis T, Zachariadis GA, Stratis JA (1997) Uptake of heavy metals by living and dead *Cladonia thalli*. *Environ Exp Bot* 37:39–52
- Chettri MK, Cook CM, Vardaka E, Sawidis T, Lanaras T (1998) The effect of Cu, Zn and Pb on the chlorophyll content of the lichens *Cladonia conculata* and *Cladonia rangiformis*. *Environ Exp Bot* 39:1–10
- Daneshvar E, Zarrinmehra MJ, Hashtjin AM, var Farhadian O, Bhatnagar A (2018) Versatile applications of freshwater and marine water microalgae in dairy wastewater treatment, lipid extraction, and tetracycline biosorption. *Bioresour Technol* 268:523–530
- De Rossi A, Rigon MR, Zapparoli M, Braidò RD, Colla LM, Dotto GL, Piccin JS (2018) Chromium (VI) biosorption by *Saccharomyces cerevisiae* subjected to chemical and thermal treatments. *Environ Sci Pollut Res* 25:19179–19186
- Ekmeçyapar F, Aslan A, Bayhan YK, Cakici A (2006) Biosorption of copper(II) by nonliving lichen biomass of *Cladonia rangiformis* hoffm. *J Hazard Mater* 137(1):293–298
- El-Moselhy MM, Ates A, Çelebi A (2017) Synthesis and characterization of hybrid iron oxide silicates for selective removal of arsenic oxyanions from contaminated water. *J Colloid Interface Sci* 488:335–347
- Gurbanov R, Unal D (2019) The biomolecular alterations in *Cladonia conculata* in response to lead exposure. *Spectrosc Lett* 51:563–570. <https://doi.org/10.1080/00387010.2018.1533564>
- He J, Chen JP (2014) A comprehensive review on biosorption of heavy metals by algal biomass: materials, performances, chemistry, and modeling simulation tools. *Bioresour Technol* 160:67–78
- Helferich F (1962) Ion exchange. McGraw Hill, New York, p 166
- Kılıç Z, Atakol O, Aras S, Cansaran-Duman D, Emregül E (2014) Biosorption properties of zinc(II) from aqueous solutions by *Pseudevernia furfuracea* (L.) Zopf. *J Air Waste Manage Assoc* 64(10):1112–1121
- Kumari P, Sharma P, Srivastava S, Srivastava MM (2006) Biosorption studies on shelled *Moringa oleifera* Lamarck seed powder: removal and recovery of arsenic from aqueous system. *Int J Miner Process* 78:131–139
- Lima Eder C et al (2019) A critical review of the estimation of the thermodynamic parameters on adsorption equilibria. Wrong use of equilibrium constant in the Van't Hoff equation for calculation of thermodynamic parameters of adsorption. *J Mol Liq* 273:425–434
- Mnif I, Fendri R, Ghribi D (2015) Malachite green bioremoval by a newly isolated strain *Citrobacter sedlakii* RI11; enhancement of the treatment by biosurfactant addition. *Water Sci Technol* 72:1283–1293
- Mnif I, Maktouf S, Fendri R, Kriaa M, Ellouze S, Ghribi D (2016) Improvement of methyl orange dye biotreatment by a novel isolated strain, *Aeromonas veronii* GRI, by SPB1 biosurfactant addition. *Environ Sci Pollut Res* 23:1742–1754
- Nash H (2008) Lichen biology. Cambridge University Press, pp 5–6
- Rodrigues DAS, Moura JM, Dotto GL, Cadaval TRS Jr, Pinto LAA (2018) Preparation, characterization and dye adsorption/reuse of chitosanvanadate films. *J Polym Environ* 26:2917–2924
- Saleh TA, Danmaliki GI (2016) Adsorbent desulfurization of dibenzothiophene byfuels by rubber tire-derived carbons: kinetics and isotherms evaluation. *Process Saf Environ Prot* 102:9–19
- Salehi P, Tajabadi FM, Younesi H, Dashti Y (2014) Optimization of Lead and nickel biosorption by *Cystoseira trinodis* (brown algae) using response surface methodology. *Clean-Soil Air Water* 42(3):243–250
- Salman SM, Ali A, Khan B, Iqbal M, Alamzeb M (2019) Thermodynamic and kinetic insights into plant-mediated detoxification of lead, cadmium, and chromium from aqueous solutions by chemically modified *Salvia moorcroftiana* leaves. *Environ Sci Pollut Res* 26:14339–14349. <https://doi.org/10.1007/s11356-019-04611-6>
- Şimşek S (2016) Adsorption properties of lignin containing bentonite–polyacrylamide composite for UO_2^{2+} ions. *Des Water* 9:1–10
- Slobodan KM (2007) A consideration of the correct calculation of thermodynamic parameters of adsorption. *J Serb Chem Soc* 72:1363–1367
- Uluozlu OD, Sari A, Tuzen M, Soylak M (2008) Biosorption of Pb(II) and Cr(III) from aqueous solution by lichen (*Parmelina tiliaceae*) biomass. *Bioresour Technol* 99(8):2972–2980
- WHO Pb^{2+} in drinking-water. Background document for development of WHO Guidelines for Drinking-Water Quality, Geneva, World Health Organization (2003) (WHO/SDE/WSH/03.04/09)
- Yazici K, Aslan A (2006) Distribution of epiphytic lichens and air pollution in the city of Trabzon, Turkey. *Bull Environ Contam Toxicol* 77(6):838–845

Publisher's note Springer Nature remains neutral with regard to jurisdictional claims in published maps and institutional affiliations.